Title : Is adaptation limited by mutation? A timescale-dependent effect of genetic diversity on the adaptive substitution rate in animals

Authors : Rousselle M[1], Simion P[1,2], Tilak MK[1], Figuet E[1], Nabholz B[1], Galtier N[1].

[1]ISEM, Univ. Montpellier, CNRS, EPHE, IRD, Montpellier, France.

[2]LEGE, Department of Biology, University of Namur, 5000 Namur, Belgium.

Corresponding author: Marjolaine Rousselle

marjolaine.rousselle@umontpellier.fr

ABSTRACT

Whether adaptation is limited by the beneficial mutation supply is a long-standing question of evolutionary genetics, which is more generally related to the determination of the adaptive substitution rate and its relationship with the effective population size N_e. Empirical evidence reported so far is equivocal, with some but not all studies supporting a higher adaptive substitution rate in large-N_e than in small-N_e species.

We gathered coding sequence polymorphism data and estimated the adaptive amino-acid substitution rate ω_a, in 50 species from ten distant groups of animals with markedly different population mutation rate θ. We reveal the existence of a complex, timescale dependent relationship between species adaptive substitution rate and genetic diversity. We find a positive relationship between ω_a and θ among closely related species, indicating that adaptation is indeed limited by the mutation supply, but this was only true in relatively low-θ taxa. In contrast, we uncover a weak negative correlation between ω_a and θ at a larger taxonomic scale. This result is consistent with Fisher's geometrical model predictions and suggests that the proportion of beneficial mutations scales negatively with species' long-term N_e.

Key words: adaptive substitution rate, beneficial mutations, effective population size, Mc-Donald and Kreitman, animals.

INTRODUCTION

It is widely recognized that adaptation is more efficient in large populations. Firstly, large populations produce a greater number of mutants per generation than small ones, and for this reason are more likely to find the alleles required for adaptation, if missing from the gene pool. Secondly, large populations tend to be genetically more diverse and thus more likely to carry the alleles needed to respond to environmental changes (1). Lastly, the fixation probability of beneficial mutations is higher in large than in small populations due to the weaker effect of genetic drift in the former. So, whether it be from standing variation or *de novo* mutations, one would expect to observe a higher rate of accumulation of adaptive changes, on average, in large than in small populations (2). Under a simple population genetic model, in a population of effective size N_e, mutations of selection coefficient $s >> 1/N_e$ should accumulate at rate $\sim 4N_e\mu_a s$ if s is small, where μ_a is the adaptive mutation rate – i.e., the adaptive substitution rate should scale linearly with $N_e\mu$ (where μ is the total mutation rate) (3).

This rationale implicitly assumes that the rate of adaptation is limited by the supply of new mutations, i.e., the population mutation rate $\theta=4N_e\mu$ (4). It might be, however, that the amount of genetic diversity available in all or most existing populations is sufficient for adaptation, and/or that the ability to adapt to environmental changes is determined in the first place by factors independent from the effective population size, such as the magnitude or frequency of perturbations, the finite set of possible genotypes an organism could reach, or the ability of populations to combine favorable alleles across loci via recombination (5–10). Finally, this rationale makes the assumption of a constant distribution of the fitness effect (DFE) across species, whereas it has been suggested that the adaptive mutation rate, μ_a, might be negatively correlated with N_e, which further complicates the situation. This is because small populations tend to accumulate deleterious mutations, and the resulting load could offer the opportunity for adaptive, compensatory mutations to arise and spread irrespective of environmental perturbations (9). Theoretical models can therefore predict a positive, negative, or lack of relationship between the population size and the adaptive substitution rate, depending on the underlying assumptions.

Molecular data offer an unique opportunity to empirically evaluate the correlation between the adaptive substitution rate and θ, and thus to test whether adaptation is actually limited by mutation.

More efficient adaptation in large populations should be reflected by an increased protein evolutionary rate, which can be estimated from coding sequence alignments. The ratio of non-synonymous (i.e. amino-acid changing, dN) to synonymous (i.e. amino-acid conservative, dS) substitution rates, often called ω, is a measure of the protein evolutionary rate that controls for the effects of the divergence time and mutation rate. However, ω is influenced by adaptation but also by the strength and efficiency of purifying selection against deleterious alleles. To account for this, McDonald and Kreitman (1991, MK) (10) suggested including within-species polymorphism in the analysis. Adaptive mutations are expected to contribute negligibly to the pool of segregating alleles. The ratio of non-synonymous to synonymous polymorphism, therefore, provides an estimator of the expected ω under neutrality, i.e., in absence of adaptation, called ω_{na} (for non-adaptive). Subtracting the neutral expectation ω_{na} from the observed ω provides an estimator of the adaptive rate, ω_a, and the proportion of adaptive substitutions, α (11).

Subsequent improvements in the MK method were intended to account for a number of factors that could potentially confound the estimation of ω_{na}, including the prevalence of slightly deleterious segregating alleles and recent demographic effects (14–21). Improved methods explicitly model the DFE of non-synonymous mutations, while taking information not only from the number of synonymous and non-synonymous single nucleotide polymorphisms (SNPs), but also from the distribution of allele frequencies across SNPs – so-called site frequency spectra (SFS). The ω_a statistics has a high sampling variance (22) and its estimation can be biased by various factors, such as a fluctuating population size (12,23,24) and GC-biased gene conversion (25–27). In particular, one key assumption of the MK approach is that the long-term N_e, which determines ω, is equal to the short-term N_e and can therefore be estimated from polymorphism data. It appears unlikely that this is generally true, and ancient fluctuations in N_e could in principle fault the MK rationale (12,23,24). Eyre-Walker (24) theoretically considered the problem of a single ancient change in N_e and showed that an expansion in population size, even if old, could lead to overestimation of the adaptive substitution rate. This bias could create spurious positive correlation between ω_a and N_e, which should be kept in mind when interpreting this type of estimate.

The first applications of the MK method to large-scale data sets indicated that the adaptive rate is higher in *Drosophila* than in humans (11,13,14). This is consistent with the prediction of more efficient adaptation in large populations and with the hypothesis that mutation limits adaptation.

These studies were, however, focused on the $\alpha=\omega_a/(\omega_a+\omega_{na})$ statistics, i.e., the proportion of amino-acid substitutions that result from adaptation. α is influenced by ω_{na} as well as ω_a, and a lower α in humans than in *Drosophila* might mainly reflect a higher rate of non-adaptive amino-acid substitution in the former. Indeed, purifying selection against deleterious mutations is likely less effective in small populations due to increased genetic drift (28). Comparative studies focused on ω_a have only revealed tenuous positive effects of θ on the adaptive rate in mammals, flies and plants (29–31). The largest scale analysis of this sort used 44 pairs of non-model species of animals occupying a wide range of θ (18). This latter study reported a significantly positive relationship between θ-related life history traits and α, consistent with previous literature, but this was entirely due to the non-adaptive component. Galtier (18) failed to detect any effect of θ on ω_a, despite using various models for the distribution of fitness effects and accounting for a number of potential confounding factors. This result did not support the hypothesis that adaptation is limited by mutation.

So, the evidence so far regarding the relationship between the adaptive substitution rate and the population mutation rate is equivocal. Existing comparative studies have involved distinct methodological approaches, both in terms of species sampling and adaptive substitution rate estimation. In particular, these studies were conducted at different evolutionary scales, which might partially explain their somewhat discordant results. In the short term, an increase in N_e is expected to boost the adaptive substitution rate if the mutation supply is limiting. In the long run, differences in N_e could also lead to changes in the DFE, and particularly in the proportion of beneficial mutations, due to the fact that small-N_e species may be pulled away from their fitness optimum via genetic drift (11,18,32). How these two opposing forces interact and combine to determine the relationship between ω_a and θ is still unknown, in the absence of a multi-scale study.

In this study, we test the effects of the evolutionary time-scale on the relationship between the adaptive substitution rate (ω_a) and the population mutation rate (θ). We gathered coding sequence polymorphism data in 4-6 species from each of ten distant groups of animals with markedly different θ. Our results reveal that the relationship between ω_a and θ varies depending on the considered taxonomic scale, i.e. depending on whether we compare closely related species or distantly related taxa. We report a positive relationship between ω_a and θ within groups, and the strength of this relationship weakens as θ increases, indicating that adaptation is limited by

beneficial mutations in small-θ animal species. At a larger taxonomic scale, in contrast, we find a weak negative correlation between ω_a and θ, with, for instance, primates and ants showing a higher adaptive substitution rate than mussels and fruit flies. This is in line with the hypothesis that long-term N_e influences the DFE, and particularly the proportion of adaptive mutations.

RESULTS

1. Data sets

We assembled a data set of coding sequence polymorphism in 50 species from ten taxonomic groups, each group including 4 to 6 closely-related species (**Table S1**). The ten taxa we analyzed were Catharrhni (Mammalia, hereafter called "primates"), Passeriformes (Aves, hereafter called "passerines"), Galloanserae (Aves, hereafter called "fowls"), Muroidea (Mammalia, hereafter called "rodents"), Lumbricidae (Annelida, hereafter called "earth worms"), *Lineus* (Nemertea, hereafter called "ribbon worms"), *Mytilus* (Mollusca, hereafter called "mussels"), Satyrini (Lepidoptera, hereafter called "butterflies"), *Formica* (Hymenoptera, hereafter called "ants"), and *Drosophila* (hereafter called "flies").

Data for five groups (primates, passerines, fowls, rodents and flies) were obtained from public databases. Data for the other five groups were newly generated via exon capture in a total of 242 individuals from 22 species (**Table 1**) and we obtained sufficient data for 216 of them (~89%). The average coverage was of 9X in ants, 23X in butterflies, 10X in earth worms, 28X in ribbon worms and 26X in mussels (average of median coverage per species). The percentage of targeted coding sequences for which at least one contig was recovered ranged from 31.9% (for *Lumbricus terrestris*, the species with the maximal divergence from the species used to design the baits) to 88.2% across species (median=78.8%, **Table 1**).

Species	Group	Targeted transcripts	Recovered transcripts	Percentage of recovered among targeted transcripts
Formica fusca	ants	1810	1427	78.8
Formica sanguinea	ants	1810	1396	77.1
Formica pratensis	ants	1810	1398	77.2
Formica cunicularia	ants	1810	1406	77.7
Maniola jurtina	butterflies	2235	1921	86.0
Melanargia galathea	butterflies	2235	1713	76.6
Pyronia tithonus	butterflies	2235	1823	81.6
Pyronia bathseba	butterflies	2235	1864	83.4
Aphantopus hyperanthus	butterflies	2235	1772	79.3
Allolobophora chlorotica L1	earth worms	2955	2293	77.6
Allolobophora chlorotica L2	earth worms	2955	2315	78.3
Allolobophora chlorotica L4	earth worms	2955	1732	58.6
Aporrectodea icterica	earth worms	2955	2321	78.5
Lumbricus terrestris	earth worms	2955	943	31.9
Lineus sanguineus	ribbon worms	1725	1251	72.5
Lineus ruber	ribbon worms	1725	1521	88.2
Lineus lacteus	ribbon worms	1725	1516	87.9
Lineus longissimus	ribbon worms	1725	1505	87.2
Mytilus galloprovincialis	mussels	2181	1820	83.4
Mytilus edulis	mussels	2181	1721	78.9
Mytilus trossulus	mussels	2181	1740	79.8
Mytilus californianus	mussels	2181	1808	82.9

Table 1: Summary of the number of targeted transcripts recovered in the capture experiment.

We assessed contamination between samples from distinct species using CroCo (33). Overall, the inter-groups connection in **Figure S1** indicates a low level of cross-contamination: when there were connections between taxonomic groups, on average they concerned 38 contigs identified as contaminants, with the worst case being the 172 contigs identified as contaminants between the assembly of *Lineus sanguineus* and *Mytilus galloprovincialis*. Connections between assemblies from closely related species were very likely false positive cases, especially since the intensity of the within-group connections was congruent with the phylogenetic distance between species within

taxa. Regardless, all contigs identified as potential contaminants were excluded from the dataset in downstream analyzes as a cautionary measure.

Within each group, we focused on orthologous contigs (**Table S2**), predicted open reading frames, and called the diploid genotypes of individuals for every coding position. The SNPs counts obtained after genotyping are summarized in **Table S3**. We obtain less than a thousand SNPs in only two species, the minimum being 153 for *Lineus longissimus*, in which we were only able to recover data for six individuals. We recovered an average of 8,459 SNPs per species in ants, 7,950 in butterflies, 4,763 in earth worms, 8,347 in ribbon worms, 19,750 in mussels, 10,191 in primates, 25,534 in rodents, 40,870 in passerines, 8,488 in fowls and 195,398 in flies.

In conclusion, the capture experiment seems suitable for recovering population coding sequence data for several closely related species - here, the maximum divergence between species within a taxonomic group was 0.2 subst./site, i.e. the divergence between *Lumbricus terrestris* and *Allolobophora chlorotica L1*.

2. Between-groups relationship between the population mutation rate (θ) and the adaptive substitution rate (ω_a)

We used Galtier's (2016) version of the MK method (18) introduced by Eyre-Walker and Keightley (2009) (16), accounting for the effect of slightly beneficial non-synonymous mutations (see Methods). Two strategies were adopted to combine SFS information from distinct species in a group-level estimate of ω_a, thus accounting for the problem of phylogenetic non-independence between species. For both strategies, we first calculated the dN/dS ratio ω at the group-level, i.e., by averaging across all branches of the tree (see Material and Methods). Our first estimator, which we called $\omega_{a[P]}$, was obtained by pooling SFS from distinct species within a group, separately for synonymous and non-synonymous SNPs (as in (34)), before fitting the model and estimating the parameters. This estimate combines data across species weighting each species equally, thus alleviating the effect of species-specific demographic history.
We then computed the relationship between $\omega_{a[P]}$ estimates and the across-species average nucleotide diversity, π_s, which was taken as an estimate of θ. We detected a significant negative relationship

between $\omega_{a[P]}$ and the across-species average nucleotide diversity, π_s, taken as an estimate of θ (regression test, r^2=0.4, p-value=2.9e-02) (**Figure 1A**).

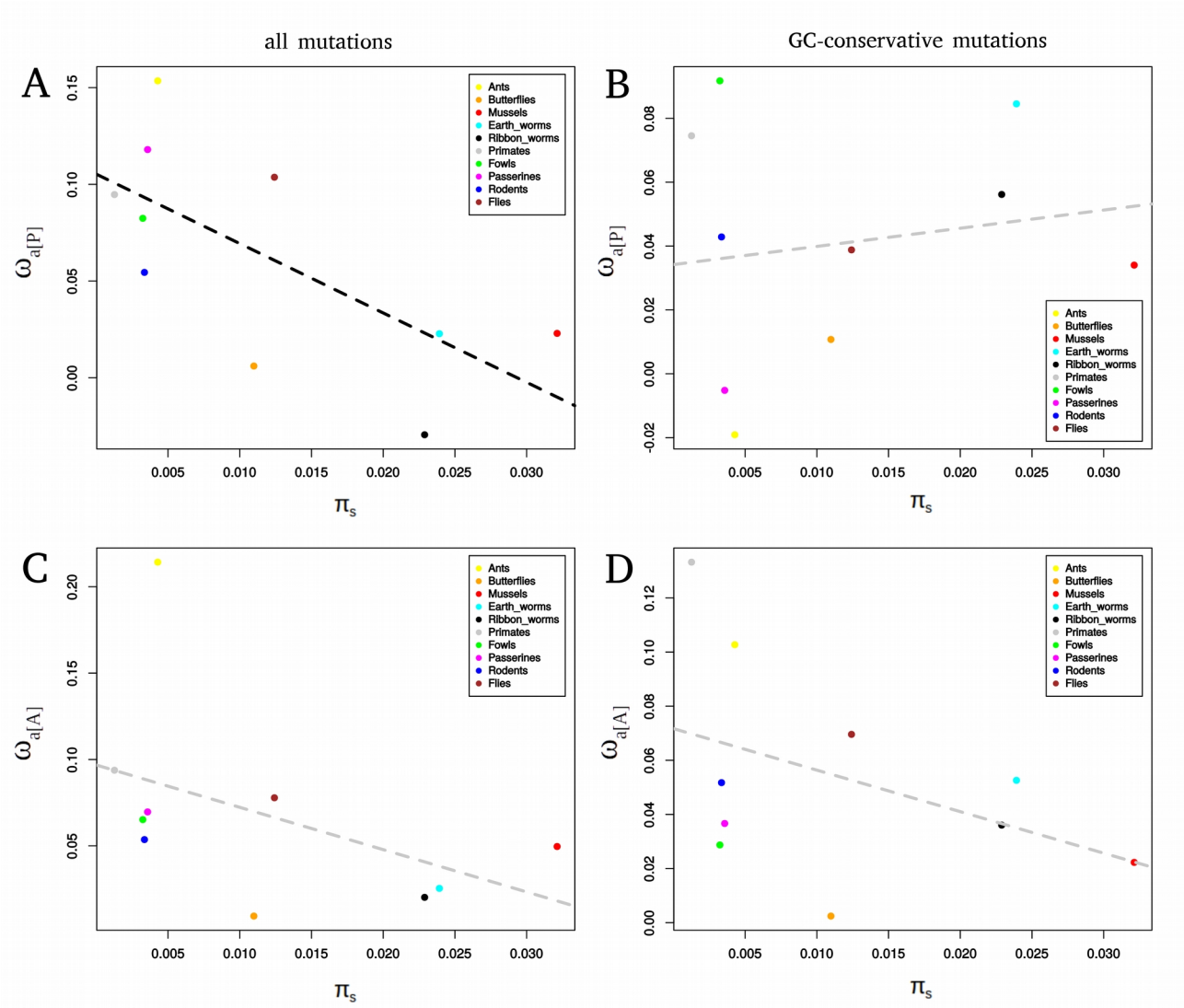

Figure 1: Relationship between group-level ω_a and group-level π_s.

A: ω_a was estimated by pooling SFS across species within a group ($\omega_{a[P]}$) using all mutations.

B: ω_a was estimated by pooling SFS across species within a group ($\omega_{a[P]}$) using only GC-conservative mutations.

C: ω_a was estimated via the averaging of ω_{na} across species within a group ($\omega_{a[A]}$) using all mutations.

D: ω_a was estimated via the averaging of ω_{na} across species within a group ($\omega_{a[A]}$) using only GC-conservative mutations.

Group level π_s was estimated by averaging species-level π_s across closely related species. Black dotted lines represent significant regressions across taxonomic groups and grey dotted lines non-significant ones.

Recent studies in birds and more recently primates indicated that GC-biased gene conversion (gBGC) may lead to overestimation (25,26) or underestimation of ω_a (27). Interestingly, gBGC does not affect genomic evolution with the same intensity in all organisms (35). To avoid bias in the estimation in species where gBGC is active, we restricted the SNP and substitution data to GC-conservative changes, which are not influenced by gBGC. We found a non-significant positive correlation $\omega_{a[P]GC\text{-}conservative}$ and θ (**Figure 1B**).

Our second estimator of the adaptive rate at the group level, which we called $\omega_{a[A]}$, was obtained by calculating the across-species arithmetic mean of ω_{na} within a group, and by then subtracting this average from ω. We suggest that $\omega_{a[A]}$ is a reasonable estimator of the adaptive rate with fluctuating population size if the pace of fluctuations is sufficiently slow, such that the sampled species have reached the selection/drift equilibrium (Supplementary Material **Box S1**). We found a non-significant negative correlation between $\omega_{a[A]}$ and $\omega_{a[A]GC\text{-}conservative}$ and π_s (**Figure 1C and 1D**). Overall, the between-group analysis seems to confirm the absence of a positive relationship between ω_a and θ at the between-phyla scale in animals, and even suggests the existence of a weak, negative relationship.

3. Relationship between life history traits and ω_a

We used several life history traits known to be correlated with species long-term effective population size (36). In our data set, all life history traits were correlated with π_s (Spearman correlation p-value, propagule size: 1.1e-12, adult size: 4.3e-04, longevity: 5.5e-02, body mass: 4.7e-03, fecundity: 9.4e-06). When estimating the per-group ω_a, we did not find any significant relationship with life history traits, but the signs of the correlation coefficients were indicative of a negative relationship between the long-term N_e and both ω_a and $\omega_{a[GC\text{-}conservative]}$ (**Figures S2 and S3**). When considering all 50 species (i.e. without controlling for phylogenetic inertia) and all mutations, we found a negative relationship between ω_a and $\log_{10}$ transformed fecundity (regression test, r^2=0.094), as well as a positive relationship with $\log_{10}$ transformed longevity (regression test, r^2=0.10) and $\log_{10}$ transformed propagule size (regression test, r^2=0.13) (**Figure 2A**). When using only GC-conservative mutations, the relationships were similar (regression test, r^2=0.11) (**Figure 2B**).

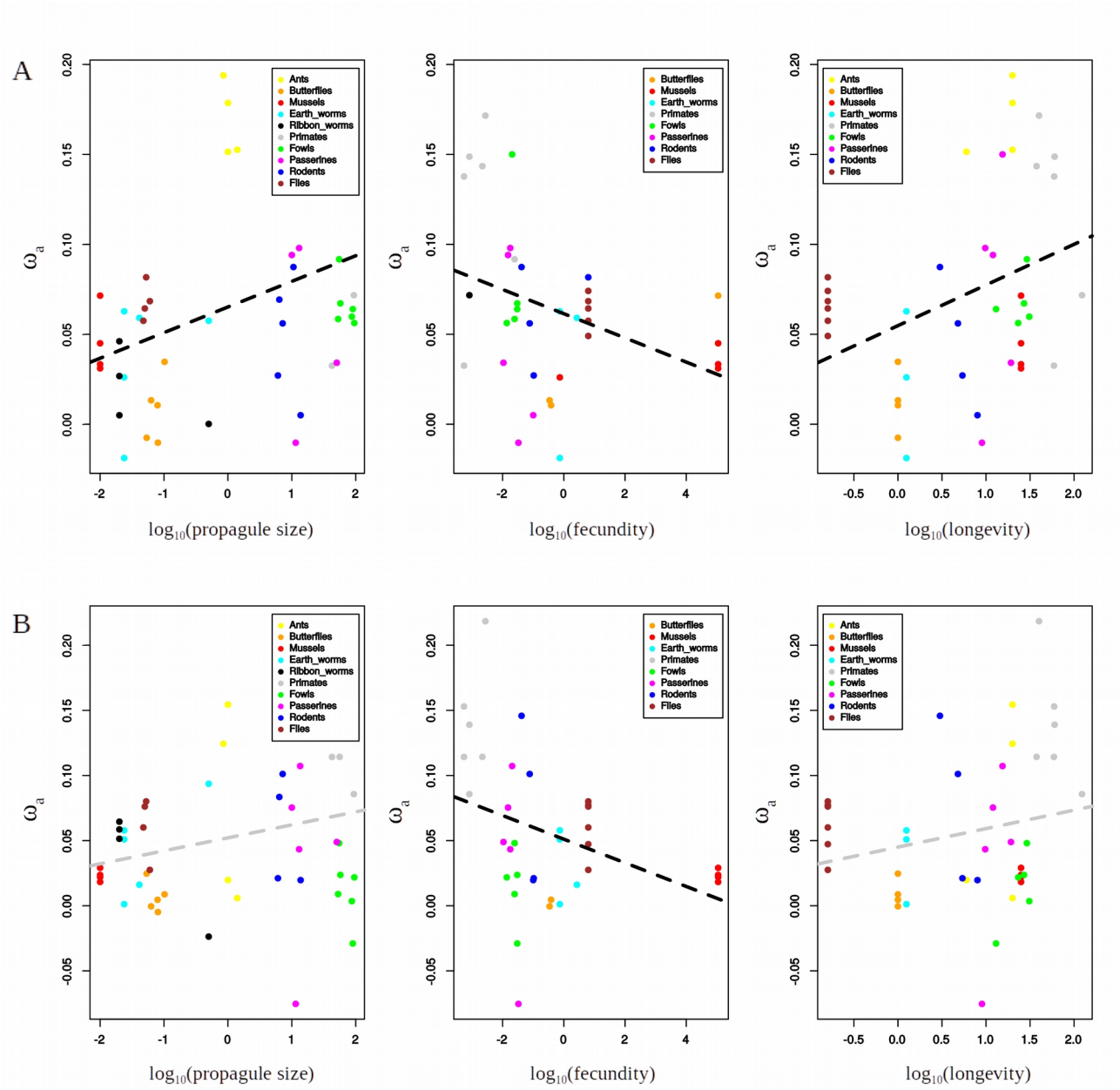

Figure 2: Relationship between species-level ω_a and life history traits.

A: ω_a is estimated using all mutations.

B: ω_a is estimated using only GC-conservative mutations.

Black dotted lines represent significant regressions across taxonomic groups and grey dotted lines non-significant ones.

We also found a negative relationship between ω_{na} and fecundity (regression test r^2=0.31), and a positive relationship between ω_{na} and propagule size (regression test r^2=0.13) and body mass (regression test r^2=0.10), which was also true when using only GC-conservative mutations: positive relationships between $\omega_{na[GC\text{-}conservative]}$ and propagule size (regression test r^2=0.21), longevity

(regression test r^2=0.12), body mass (regression test r^2=0.08) and a negative relationship with fecundity (regression test r^2=0.36) (**Figure S4**).

4. Within-group relationship between θ and ω_a

To assess the within-group effect of π_s on ω_a, we performed an analysis of covariance (ANCOVA) with the taxonomic group as a categorical independent variable, as in (29). The principle of this analysis is to fit a set of parallel lines (one for each taxonomic group) and test whether their common slope is significantly different from zero. Moreover, we tested if the relationship between ω_a and π_s or life history traits differs between taxonomic groups by testing whether the lines have different intercepts.

By this strategy, we found that ω_a and both π_s and $\log_{10}(\pi_s)$ were significantly positively correlated when using only GC-conservative mutations (ANCOVA p-value=2.8e-02 and 3.1e-03, respectively) (**Figure 3B**). ω_a was only marginally positively correlated with $\log_{10}(\pi_s)$ when using all mutations (ANCOVA p-value=7.6e-02) (**Figure 3A**). We also found that there was a significant variation between the intercepts (ANCOVA p-value<1e-03), as well as a significant interaction between the dependent variable and the categorical independent variable (ANOVA p-value=1.6e-02). Those results support the existence of a positive relationship between ω_a and θ within groups, with the slope of the relationship differing between groups. This is consistent with the hypothesis that within a group, higher-θ species are more likely to find and fix adaptive substitutions than low-θ species, in line with the hypothesis that mutation limits adaptation. **Figure 3** shows that the slopes of the within-group ω_a/θ correlations decreased with group-level π_s, and we actually found a significant negative correlation between these two quantities both when using all or only GC-conservative mutations (Spearman correlation coefficient=-0.77, p-value=1.4e-02). This interestingly suggests that the limitation of adaptation by the supply of adaptive mutations is effective and strong in small-θ groups (e.g. primates, rodents, ants), but not in high-θ groups of animals (e.g. flies, mussels, butterflies), where the ω_a/θ relationship is essentially flat (**Figure 3**).

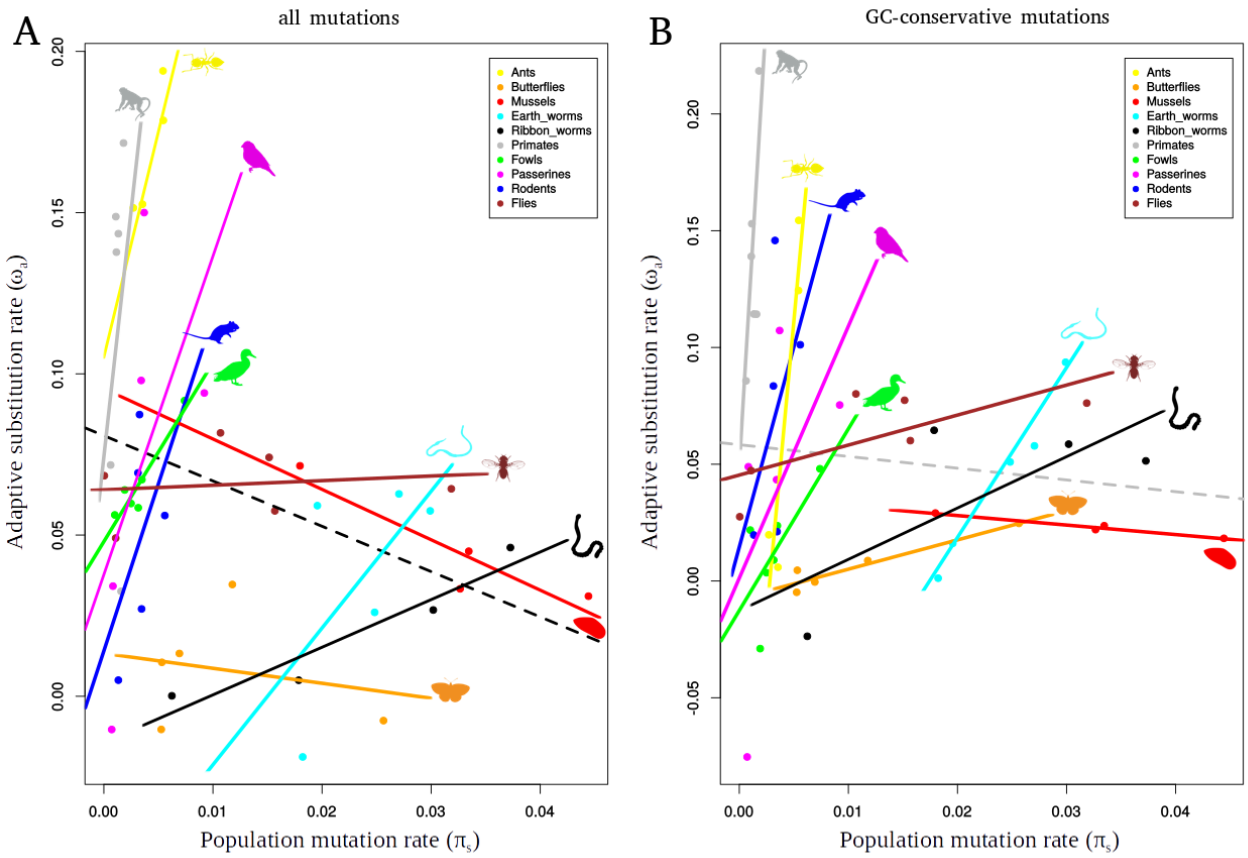

Figure 3: Relationship between species-level ω_a and π_s.

A: ω_a is estimated using all mutations.

B: ω_a is estimated using only GC-conservative mutations.

Black dotted lines represent significant regressions across taxonomic groups and grey dotted lines non-significant ones.

When analyzing the per-species non-adaptive substitution rate, we found a global negative relationship between ω_{na} and π_s (using both all mutations and only GC-conservative mutations: regression test r^2=0.16 and r^2=0.33, respectively), and a significantly negative relationship within groups (ANCOVA p-value=1.9e-02 and p-value=1.8e-03, respectively) (**Figure S4**). This was consistent with the expectations of the nearly neutral theory of evolution (28), and with previous empirical results (18,37). The estimated ratio of adaptive to total non-synonymous substitutions, α, behaved more or less similarly to ω_a (**Figure S5**).

5. Control for fluctuations in N_e

We were concerned that the positive correlation between ω_a and π_s might have been due to an artifact generated by past fluctuations in population size (23,24). To test this, we simulated coding sequence evolution under several demographic scenarios with four regimes of demographic fluctuations, with a three or thirty-fold ratio between the low and high N_e, and a high or low long-term N_e (see Material and Method and **Figure S6**). We found that the only scenario where demographic fluctuations could lead to a detectable positive correlation between ω_a and π_s was that with the highest long-term N_e and highest difference between the low and high N_e (see **Figure S7 panel B,** regression test r^2=0.07, p-value=9.5e-03). The correlation disappeared when we used a ten-fold smaller long-term N_e, whereas we empirically observed that the correlation between ω_a and π_s was stronger for small long-term N_e groups (**Figure 2**). These simulations therefore suggested that ancient demographic fluctuations could not explain our finding of a positive within-group correlation between ω_a and π_s in low-θ groups. We also checked that the F_{is} statistics was not significantly correlated to ω_a (regression test p-value=5.9e-01) or π_s (p-value=2.9e-01), which indicated that population substructure was unlikely to confound our results.

DISCUSSION

1. Influence of θ on ω_a : a two-scale mechanism

In this study, we analyzed a 50-species population genomic data set to assess the relationship between the adaptive substitution rate and the population mutation rate and test the hypothesis that mutation limits adaptation in natural populations of animals.

We found that the relationship between ω_a and θ depended on the considered timescale, which is expected if the assumption of a fixed DFE across divergent taxa does not hold. At a recent evolutionary scale (i.e., neutral divergence <0.2 subst./site), we found a significant positive correlation between ω_a and π_s (**Figure 2**). Interestingly, the slope of the relationship differed significantly among taxonomic groups, and this slope itself was negatively correlated with the group average π_s. Otherwise, estimates at the group level revealed a weak but consistently negative relationship between ω_a and π_s, and between ω_a and various life history traits correlated with the

long-term N_e (**Figure 1** and **3**). This time scale-dependent behavior of the ω_a/θ relationship was here demonstrated via the analysis of a single, multi-scale dataset, somehow reconciling earlier taxon-specific studies on the subject (4,8,18,29–31,38).

2. Relationship between θ and ω_a - a real causative link or an artifact ?

Our ANCOVA analysis revealed that the slopes of the relationships between ω_a and π_s within each taxonomic group were significantly different from zero, demonstrating the existence of a positive link between ω_a and π_s within groups (**Figure 2**). We were concerned that this relationship may have resulted from a bias in the MK approach, instead of being a true biological signal. Indeed, the MK approach implicitly assumes that the regime of selection/drift has been constant over the considered time period, i.e. since the divergence between the focal and outgroup species. If however the selection/drift regime had changed (e.g. via a change in effective population size) between the period during which divergence had accumulated and the period during which polymorphism was built, this could lead to overestimation or underestimation of ω_a (23,24). Here, we used the so-called r_i's nuisance parameters (39) to control for recent changes in N_e.

In contrast, ancient N_e changes that affect coding sequence divergence are virtually impossible to trace. We showed in a previous simulation-based study that ancient demographic fluctuations could lead to severely overestimated α and ω_a - an upward bias which is exacerbated when the true adaptive substitution rate is low (23). Moreover, it has been shown by modeling single changes in N_e that in the presence of slightly deleterious mutations, an increase in N_e in the past could yield spurious evidence of positive selection, which can lead to a spurious positive correlation between ω_a and π_s (24).

We used simulations to test if demographic fluctuations could lead to such a correlation. Our results suggested that long-term fluctuations were not responsible for the positive link between ω_a and π_s that we report. In addition, the gradual decrease in the slope of the relationship with per-group average π_s was also consistent with the fact that the relation is genuine, because (i) we do not expect the demographic fluctuation regime to correlate with the average π_s of the group, and (ii) there was no relationship between the inter-group variation in π_s and the average π_s of the group (Spearman correlation test: p-value=4.7e-01).

A recently developed method allows the estimation of α and ω_a using polymorphism data alone (20), thus avoiding the assumption of time constancy of the drift/selection regime. However, estimates of α and ω_a by this method deserve a specific interpretation, as they represent the rate of adaptive evolution of the species during its very recent history, and not the one of its long-term history. This method requires high quality datasets and highly polymorphic species, and it was not applicable to our dataset, in which species and groups differ widely in terms of SNP numbers (**Table S3**).

3. Mutation limits adaptation within taxonomic groups in small-θ animals

Our findings therefore indicate of a genuine link between the adaptive substitution rate and θ, which is consistent with the hypothesis that, in several groups of animals, the rate of adaptation is limited by the supply of beneficial mutations. The slope of the relationship was particularly steep in ants, fowls, passerines, rodents and primates (**Figure 2**). For instance, the estimated adaptive rate in rhesus macaque (*Macaca mulatta*: π_s=0.0018) was more than 3-fold higher than that of humans (*Homo sapiens*: π_s=0.0006). Note that this interpretation relies on the assumption that different species from a given taxonomic group share the same DFE and, in particular, the same proportion of beneficial mutations. This is consistent with previous analyses of the relationship between ω_a and π_s at a relatively recent time scale (27,29). It is also consistent with the finding that strong selective sweeps are more abundant in species of great apes with a large population size (4).

Interestingly, we found that the relationship between ω_a and π_s was significantly stronger in low-diversity than high-diversity groups. In flies, a high-diversity group, the slope of the linear regression between the two variables was only 1.3, whereas it was between 7.8 and 77 in the four vertebrate groups. In mussels, i.e. the taxonomic group with the highest average diversity in our dataset, we detected no significant relationship between ω_a and π_s, with the slope being very close to zero (-0.4). It is possible that in such organisms the adaptive evolutionary rate is not limited by the mutation supply: the standing variation and/or the influx of new mutations are sufficient for proteins to find the required alleles. This is consistent with the results of (8), who showed that patterns of adaptation to insecticides in natural *Drosophila melanogaster* populations are incompatible with the hypothesis that adaptation is mutation-limited. This is also consistent with the results of Jensen and

Bachtrog (40), who found very similar rates of adaptation between two *Drosophila* species with different N_e.

Finally, the results shown in **Figure 3** corroborate theoretical predictions indicating that when N_e is sufficiently large, it is the species ability to combine beneficial alleles across loci that limits adaption rather than the strength of selection or the mutation supply (9). Our results suggest that this situation applies to large-N_e groups of animals, such as *Drosophila*, but not to small-N_e ones, such as primates. Indeed, one should keep in mind that the two variables we analyze here, π_s and ω_a, are potentially affected by the effects of interference between segregating mutations (17). Weissman & Barton (9), following Gillespie (41), explicitly modeled linkage between beneficial mutations and showed that the effect of N_e on the adaptive rate is expected to saturate when parameters are set to values estimated in *Drosophila*. The neutral genetic diversity is also expected to be affected by linked selection (42,43), to an extent that still deserves to be properly assessed (44). Quantifying the effect of linked selection on the neutral and selected variation, and its relationship with N_e, is a current challenge and would help interpreting results such as the ones we report here.

4. What are the determinants of ω_a across distantly related taxa?

We used two approaches to estimate the adaptive substitution rate at the group level. Both supported a negative among-group relationship between ω_a and π_s, and between ω_a and life history traits that have been shown to be linked to the long-term effective population size (36) (**Figure 1, S2, S3** and **3**). As different sets of genes were used in the different groups of animals, the gene content might have influenced our results. Indeed, Enard et al. (45) showed that genes interacting with viruses experience a significantly higher adaptive substitution rate, thus demonstrating the importance of the gene sampling strategy in comparative studies. In the exon capture experiment, a subset of genes were randomly sampled from an existing transcriptome reference, whereas all available genes were used in the other species (provided that they were present in all species within a group). We do not see any particular reason why the gene sample would be biased with respect to virus interacting proteins in some specific groups, and we did not detect any effect of data type (i.e. exon capture *vs*. genome-wide) on ω_a. Our results are consistent with the results of Galtier (16), who analyzed the relationship between ω_a and π_s in a transcriptomic dataset of 44 distantly related species of animals. Indeed, the main analysis in Galtier (18) revealed no significant correlation between ω_a and π_s, but

various control analyses (particularly using GC or expression restricted datasets) yielded a significantly negative correlation between the two variables. This suggests that the mutation limitation hypothesis does not accurately account for the variation of ω_a at a large taxonomic scale,implying that factors other than θ must be at work here. Hereafter we discuss a number of such potential factors in the light of Fisher's geometrical model (FGM), which provides a convenient framework for considering the determinants of the adaptive substitution rate.

First, simulations under FGM and a moving optimum showed that the adaptive substitution rate is primarily determined by the rate of environmental change (32,46). If one assumes that species with a longer generation time undergo a higher per generation rate of environmental change, and that generation time is negatively correlated to population size in animals, then our results could perhaps be interpreted this way (36).

Moreover, Lourenço et al. (32) suggested that organismal complexity, represented by the dimensionality of the phenotypic space in FGM, affects the adaptive substitution rate more strongly than the effective population size does, with the adaptive substitution rate being an increasing function of complexity. This is because the probability that a new mutation is in the optimal direction decreases as the number of potential directions increases, such that the average adaptive walk takes more steps in a high-dimension than a low-dimension space (32,47). Complexity *sensus* FGM, however, is very hard to quantify in a biologically relevant way. To argue that primates and birds are more complex than mussels and worms does not seem particularly relevant when considering the organism level. Different measures of complexity have been considered at the molecular or cellular level, such as genome size, gene or protein number, number of protein-protein interactions, number of cell types, and these seem to point towards a higher complexity in mammals than insects, for instance (37,38). This is consistent with the idea of a greater complexity of species with smaller N_e. Fernández and Lynch (50) suggested that the accumulation of mildly deleterious mutations in small populations induces secondary selection for protein–protein interactions that stabilize key gene functions, thus introducing a plausible mechanism for the emergence of molecular complexity (50). If the number of protein-protein interactions is a relevant measure of proteome complexity, then this might contribute to explain our findings of a higher adaptive substitution rate in low-θ than in high-θ groups.

Finally, variations in ω_a across distantly related taxa could be modulated by the long-term N_e via the mean distance of the population to the fitness optimum. Indeed, under FGM, the proportion of beneficial mutations increases with the distance to the optimum. Groups of species evolving under small long-term N_e are further away from their optimum, compared to larger-N_e groups, due to an increased rate of fixation of deleterious mutations at equilibrium, so they are predicted to undergo a larger proportion of beneficial, compensatory mutations. Empirical analyses of SFS based on large samples in humans and flies are consistent with the hypothesis that humans are on average more distant to their optimum than flies (11).

To sum up, our results suggest that factors linked to species long-term effective population size affect the DFE, i.e., the proportion and rate of beneficial mutation would be non-independent of the long-term N_e. We suggest that the proteome is probably more complex and further away from its optimal state in small-N_e than in large-N_e groups of animals, which might contribute to increasing the steady-state adaptive rate in the former, thus masking the effect of mutation limitation in across-group comparisons.

CONCLUSION

In this study, we sampled a large variety of animals species and demonstrated a timescale-dependent relationship between the adaptive substitution rate and the population mutation rate, that reconciles previous studies that were conducted at different taxonomic scales. We demonstrate that the relationship between the adaptive substitution rate and θ within closely related species sharing a similar DFE is shaped by the limited beneficial mutation supply, whereas the between-group pattern probably reflects the influence of long-term population size on the proportion of beneficial mutations. Our results provide empirical evidence for mutation-limited adaptive rate at whole proteome level in small-N_e groups of animals, while stressing the fact that DFE is not independent of the long-term effective population size – a crucial factor that must be properly accounted for in large-scale comparative population genomic analyses.

MATERIAL & METHODS

1. Data set

Genomic, exomic and transcriptomic data from primates, passerines, fowls, rodents and flies were retrieved from the SRA database. Detailed referenced, bioprojects and sample sizes are provided in **Table S1**. The minimal sample size was five diploid individuals (in *Papio anubis*) and the maximum was 20 (in seven species).

Exon capture data were newly generated in ants, butterflies, mussels, earth worms and ribbon worms. We gathered tissue samples or DNA samples for at least eight individuals per species and four or five species per group. Reference transcriptomes were obtained from previously published RNA-seq data in one species per taxonomic group (36,51,52). Details of the species and numbers of individuals are presented in **Table S1**.

2. Multiplexed target capture experiment

DNA from whole animal body (ants), body section (earth worms, ribbon worms), mantle (mussels) or head/thorax (butterflies) was extracted using DNAeasy Blood and Tissue kit (QIAGEN) following the manufacturer instructions. About 3 µg of total genomic DNA were sheared for 20 mn using an ultrasonic cleaning unit (Elmasonic One). Illumina libraries were constructed for all samples following the standard protocol involving blunt-end repair, adapter ligation, and adapter fill-in steps as developed by (53) and adapted in (54).

To perform target capture, we randomly chose contigs in five published reference transcriptomes (*Maniola jurtina* for butterflies (51), *Lineus longissimus* for ribbon worms (36), *Mytilus galloprovincialis* for mussels (36), *Allobophora chlorotica L1* for earth worms (36), and *Formica cunicularia* for ants (52)) in order to reach 2Mb of total sequence length per taxon (~2000 contigs). 100nt-long baits corresponding to these sequences were synthesized by MYbaits (Ann Arbor, MI, USA), with an average cover of 3X.

We then performed multiplexed target capture following the MYbaits targeted enrichment protocol: about 5 ng of each library were PCR-dual-indexed using Taq Phusion (Phusion High-Fidelity DNA Polymerase Thermo Scientific) or KAPA HiFi (2× KAPA HiFi HotStart ReadyMix KAPABIOSYSTEMS) polymerases. We used primers developed in (55). Indexed libraries were purified using AMPure (Agencourt) with a ratio of 1.6, quantified with Nanodrop ND-800, and pooled in equimolar ratio. We had a total of 96 combinations of indexes, and two Illumina lanes, for a total of 244 individuals. This means that we had to index two (rarely three) individuals with the same combination to be sequenced in the same line. When this was necessary, we assigned the same tag to individuals from distantly related species (i.e. from different groups). Exon capture was achieved according to the Mybaits targeted enrichment protocol, adjusting the hybridization temperature to the phylogenetic distance between the processed library and the baits. For libraries corresponding to individuals from the species used to design baits, we used a temperature of 65°C during 22 h. For the other ones we ran the hybridization reactions for 16 h at 65°C, 2 h at 63°C, 2 h at 61°C and 2 h at 59°C. Following hybridization, the reactions were cleaned according to the kit protocol with 200 µL of wash buffers, and hot washes were performed at 65°C or 59°C depending on the samples. The enriched solutions were then PCR-amplified for 14 to 16 cycles, after removal of the streptavidin beads. PCR products were purified using AMPure (Agencourt) with a ratio of 1.6, and paired-end sequenced on two Illumina HiSeq® 2500 lines. Illumina sequencing and demultiplexing were subcontracted.

3. Assembly and genotyping

For RNA-seq data (i.e. fowls and two rodents), we used trimmomatic (56) to remove Illumina adapters and reads with a quality score below 30. We constructed *de novo* transcriptome assemblies for each species following strategy B in (57), using Abyss (58) and Cap3 (59). Open reading frames (ORFs) were predicted using the Trinity package (60). Contigs carrying ORF shorter than 150 bp were discarded. Filtered RNA-seq reads were mapped to this assembly using Burrow Wheeler Aligner (BWA) (version 0.7.12-r1039) (61). Contigs with a coverage across all individual below 2.5xn (where n is the number of individuals) were discarded. Diploid genotypes were called according to the method described in (62) and (63) (model M1) via the software reads2snps (https://kimura.univ-montp2.fr/PopPhyl/index.php?section=tools). This method calculates the posterior probability of each possible genotype in a maximum likelihood framework. Genotypes

supported by a posterior probability higher than 95% are retained, otherwise missing data is called. We used version of the method which accounts for between-individual, within-species contamination as introduced in (52), using the -contam=0.1 option, which means assuming that up to 10% of the reads assigned to one specific sample may actually come from a distinct sample, and only validating genotypes robust to this source of uncertainty.

For primates, rodents, passerines and flies, reference genomes, assemblies and annotations files were downloaded from Ensembl (release 89) and NCBI (**Table S1**). We kept only '*CDS*' reports in the annotations files, corresponding to coding exons, which were annotated with the automatic Ensembl annotation pipeline, and the havana team for *Homo sapiens*. We used trimmomatic to remove Illumina adapters, to trim low-quality reads (i.e. with an average base quality below 20), and to keep only reads longer than 50bp. Reads were mapped using BWA (61) on the complete reference assembly. We filtered out hits with mapping quality below 20 and removed duplicates, and we extracted mapping hits corresponding to regions containing coding sequences according to the annotated reference assembly. This was done to avoid calling SNPs on the whole genome, which would be both time consuming and useless in the present context. We called SNPs using a pipeline based on GATK (v3.8-0-ge9d80683). Roughly, this pipeline comprised two rounds of variant calling separated by a base quality score recalibration. Variant calling was first run on every individuals from every species using HaplotypeCaller (--emitRefConfidence GVCF --genotyping_mode DISCOVERY -hets 0.001). The variant callings from all individuals of a given species were then used to produce a joint genotype using GenotypeGVCFs. Indels in the resulting vcf files were then filtered out using vcftools. The distributions of various parameters associated with SNPs were then used to set several hard thresholds (i.e. Quality by Depth < 3.0; Fisher Strand > 10; Strand Odds Ratio > 3.0; MQRootMeanSquare < 50; MQRankSum < -0.5; ReadPosRankSum < -2.0) in order to detect putative SNP-calling errors using VariantFiltration. This erroneous SNPs were then used for base quality score recalibration of the previously created mapping files using BaseRecalibrator. These mappings with re-calibrated quality scores were then used to re-call variants (HaplotypeCaller), to re-produce a joint genotype (GenotypeGVCFs, --allsites) and to re-set empirical hard thresholds (i.e. same values as above, except for Quality by Depth < 5.0). The obtained vcf files were converted to fasta files (i.e. producing two unphased allelic sequences per individual) using custom python scripts while discarding exons found on both mitochondrial and sexual chromosomes and while filtering out additional SNPs: we removed SNPs with a too high

coverage (thresholds were empirically set for each species), with a too low coverage (i.e. 10x per individual) and with a too low genotype quality per individual (i.e. less than 30).

For reads generated through target capture experiment, we cleaned reads with trimmomatic to remove Illumina adapters and reads with a quality score below 30. For each species, we chose the individual with the highest coverage and constructed de novo assemblies using the same strategy as in fowls. Reads of each individuals were then mapped to the newly generated assemblies for each species, using BWA (61). Diploid genotypes were called using the same protocol as in fowls. We used a version of the SNP calling method which accounts for between-individual, within-species contamination as introduced in (52) (see the following section). As the newly generated assemblies likely contained intronic sequences, the predicted cDNAs were compared to the reference transcriptome using blastn searches, with a threshold of e-value of 10e-15. We used an in-house script to remove any incongruent correspondence or inconsistent overlap between sequences from the transcriptomic references and the predicted assemblies, and removed six base pairs at each extremity of the resulting predicted exonic sequences. These high-confidence exonic sequences were used for downstream analyses.

3. Contamination detection and removal

For the newly generated data set, we performed two steps of contamination detection. First, we used the software tool CroCo to detect inter-specific contamination in the *de novo* assembly generated after exon capture (33).

CroCo is a database-independent tool designed to detect and remove cross-contaminations in assembled transcriptomes of distantly related species. This program classifies predicted cDNA in five categories, “clean”, “dubious”, “contamination”, “low coverage” and “high expression”.
Secondly, we used a version of the SNP calling method which accounts for between-individual, within-species contamination as introduced in (52), using the -contam=0.1 option. This means assuming that up to 10% of the reads assigned to one specific sample may actually come from a distinct sample, and only validating genotypes robust to this source of uncertainty.

4. Orthology prediction and divergence analysis

In primates, we extracted one-to-one orthology groups across the six species from the OrthoMaM database (64,65).

In fowls, passerines, rodents and flies, we translated the obtained CDS into proteins and predicted orthology using OrthoFinder (66). In fowls, full coding sequences from the well-annotated chicken genome (Ensembl release 89) were added to the dataset prior to orthology prediction, then discarded. We kept only orthogroups that included all species. We aligned the orthologous sequences with MACSE (Multiple Alignment for Coding SEquences (67).

In each of earth worms, ribbon worms, mussels, butterflies and ants, orthogroups were created via a a blastn similarity search between predicted exonic sequences reference transcriptomes. In each taxon, we concatenated the predicted exonic sequences of each species that matched the same ORF from the reference transcriptome and aligned these using MACSE. We then kept alignments comprising exactly one sequence per species or if only one species was absent.
We estimated lineage specific dN/dS ratio using bppml (version 2.4) and MapNH (version 2.3.2) (68), the former for estimating each branch length and the latter for mapping substitutions on species specific branches.

Tree topologies were obtained from the literature (**Table S4**). In passerines, fowls, rodents, flies and primates, we kept only alignments comprising all the species. In the other groups we also kept alignments comprising all species but one. We also estimated dN/dS ratios at group level by adding up substitution counts across branches of the trees, including internal branches.

To account for GC-biased gene conversion, we modified the MapNH software such that only GC-conservative substitutions were recorded (26). We estimated the non-synonymous and synonymous number of GC-conservative sites per coding sequence using an in-house script. We could then compute the dN/dS ratio only for GC-conservative substitutions.

5. Polymorphism analysis

For each taxon, we estimated ancestral sequences at each internal node of the tree with the Bio++ program SeqAncestor (68). The ancestral sequences at each internal node were used to orientate single nucleotide polymorphisms (SNPs) of species that descend from this node. We computed non-synonymous (π_n) and synonymous (π_s, i.e. θ) nucleotide diversity, as well as π_n/π_s using the software dNdSpiNpiS_1.0 developed within the PopPhyl project (https://kimura.univ-montp2.fr/PopPhyl/index.php?section=tools) (using gapN_site=4, gapN_seq=0.1 and median transition/transversion ratio values estimated by bppml for each taxonomic group). We also computed unfolded and folded synonymous and non-synonymous site frequency spectra both using all mutations and only GC-conservative mutations using an in-house script as in (18).

6. Mc-Donlad-Kreitman analysis

We estimated α, ω_a and ω_{na} using the approach of (16) as implemented in (18) (program Grapes v.1.0). It models the distribution of the fitness effects (DFE) of deleterious and neutral non-synonymous mutations as a negative Gamma distribution, which is fitted to the synonymous and non-synonymous site frequency spectra (SFS) computed for a set of genes. This estimated DFE is then used to deduce the expected dN/dS under near-neutrality. The difference between observed and expected dN/dS provides an estimate of the proportion of adaptive non-synonymous substitutions, α. The per mutation rate of adaptive and non-adaptive amino-acid substitution were then obtained as following: $\omega_a = \alpha(dN/dS)$ and $\omega_{na} = (1-\alpha)(dN/dS)$. We computed these statistics for each species using the per branch dN/dS ratio, using either all mutations and substitutions, or only GC-conservative mutations and substitutions.

We used three different distributions to model the fitness effects of mutations that have been shown to perform the best in (18). Two of these models, GammaExpo and ScaledBeta, account for the existence of slightly beneficial non-synonymous mutations. We then averaged the estimates of the three models using Akaike weights as follows:

$$\overline{\alpha} = \alpha_{GammaZero} * AICw_{GammaZero} + \alpha_{GammaExpo} * AICw_{GammaExpo} + \alpha_{ScaledBeta} * AICw_{ScaledBeta}$$
$$\overline{\omega_a} = \alpha_{GammaZero} * AICw_{GammaZero} + \omega_{aGammaExpo} * AICw_{GammaExpo} + \omega_{aScaledBeta} * AICw_{ScaledBeta}$$
$$\overline{\omega_{na}} = \omega_{naGammaZero} * AICw_{GammaZero} + \omega_{naGammaExpo} * AICw_{GammaExpo} + \omega_{naScaledBeta} * AICw_{ScaledBeta}$$

where AICw stands for akaike weigths that were estimated using the akaike.weights function in R (https://www.rdocumentation.org/packages/qpcR/versions/1.4-1/topics/akaike.weights).

When estimating DFE model parameters, we accounted for recent demographic effects, as well as population structure and orientation errors, by using nuisance parameters, which correct each class of frequency of the synonymous and non-synonymous SFS relative to the neutral expectation in an equilibrium Wright–Fisher population (39).

We also estimated α, ω_a and ω_{na} at group level. Two approaches were used. Firstly, we pooled species specific SFS from each group, and used the dN/dS ratio of the total tree of each taxon. We did so following the unweighted and unbiased strategy of (34), which combines polymorphism data across species with equal weights. Briefly, we divided the synonymous and non-synonymous number of SNPs of each category of the SFS of each species by the total number of SNPs of the species, then we summed those normalized numbers across species and finally we transformed those sums so that the total number of SNPs of the pooled SFS matches the total number of SNPs across species. The resulting estimate was called $\omega_{a[P]}$. Secondly, we calculated the arithmetic mean of ω_{na} across species within a taxonomic group to obtain a non-adaptive substitution rate at the group level. We then subtracted this average from the dN/dS ratio calculating across the whole tree of each taxon to obtain an estimate of the adaptive substitution rate at group level (called $\omega_{a[A]}$).

7. Life history traits variables

Five life history traits were retrieved from the literature for each species: adult size (i.e. the average length of adults), body mass (i.e. the mean body mass of adults' wet weights), fecundity (i.e. the number of offspring released per day), longevity (i.e. the maximal recorded longevity in years), and propagule size (i.e. the size of the juvenile or egg or larva when leaving parents or group of relatives) (**Table S5**). In the case of social insects and birds, parental care is provided to juveniles until they reach adult size so in these cases, propagule size is equal to adult size.

8. Simulations

In order to evaluate whether our method to estimate the adaptive substitution rate could lead to a spurious correlation between π_s and ω_a, we simulated the evolution of coding sequences in a single population undergoing demographic fluctuations using SLIM V2 (69). We considered panmictic populations of diploid individuals whose genomes consisted of 1500 coding sequences, each of 999 base pairs. We set the mutation rate to 2.2e-9 per base pair per generation, the recombination rate to 10e-8 per base (as in (23)) and the DFE to a gamma distribution of mean -740 and shape 0.14 for the negative part, and to an exponential distribution of mean 10^{-4} for the positive part (those DFE parameters correspond to the DFE estimated from the pooled SFS of primates). We simulated several demographic scenarios with four regimes of frequency of the fluctuations, as well as four regimes of intensity of the fluctuations (see **figure S5**). We sampled polymorphism and divergence for 20 individuals at several time points during the simulations, evaluated π_s and ω_a and measured the correlation between the two variables.

Acknowledgments

We thank Roger de Vila, Lise Dupont, Nicolas Bierne and Christophe Galkowski for providing us with tissue or DNA samples. We thank Iago Bonicci for the homemade program that allowed us to remove intronic sequences of the contigs obtained during the capture experiment by identifying any incongruent correspondence or inconsistent overlap on both the transcriptomic reference and the assembly of the capture experiment contigs. We also thank Yoann Anselmetti, Thibault Leroy and Jonathan Romiguier for their frequent help, Yoann Anciaux for sharing his experience with Fisher's geometrical model predictions, and Thomas Bataillon for his pieces of advice with regards to the DFE-α method models and estimates.

This preprint has been reviewed and recommended by Peer Community In Evolutionary Biology (https://doi.org/10.24072/pci.evolbiol.100080).

Data accessibility:

Illumina raw reads of the capture experiment are deposited under the Bioproject PRJNA530965 in the SRA database.

Conflict of interest disclosure: The authors of this preprint declare that they have no financial conflict of interest with the content of this article. Nicolas Galtier is one of the PCI Evol Biol recommenders.

Supplementary tables and figures legends:

Table S1 : Details of the species used in this study and numbers of individuals for each species.

Table S2 : Number of orthogroups for each taxonomic group.

The differences in terms of number of orthogroups comes from the fact that we not only kept orthogroups with all species but also orthogroups with all species but one to estimate dN/dS value for each terminal branches in order to maximize the number of substitutions for data sets generated by exon capture.

Table S3: SNPs counts for each species.

SNPs counts are not integers because they corresponds to SNPs that are present in our SFS, where we chose a sample size (i.e. the number of categories of the SFS) lower that 2*n, where n is the number of individuals. This is to compensate the uneven coverage between individuals that results in some sites in some individuals not to be genotyped. We chose sample sizes that maximize the number of SNPs in each SFS.

Table S4: Sources of the tree topologies of each taxonomic group used to estimate branch length and map substitutions.

Table S5: Values and sources of the life history traits used in this study.

Figure S1: Cross contamination network for *de novo* assemblies from exon capture.

Circles represent the assemblies, and arrows and their corresponding numbers represent the number of cross contaminants. Most cross contamination events occur between closely-related species and are therefore likely false positive cases.

Figure S2: Relationship between $\omega_{a[P]}$ and π_s and $\log_{10}$ transformed life history traits.

$\omega_{a[P]}$ is estimated using all mutations and substitutions (A) or using only GC-conservative mutations and substitutions (B). Group level π_s and life history traits are estimated by averaging species level estimates across closely related species. Black dotted lines represent significant regressions across taxonomic groups and grey dotted lines non-significant ones.

Figure S3: Relationship between $\omega_{a[A]}$ and π_s and $\log_{10}$ transformed life history traits.

$\omega_{a[A]}$ is estimated using all mutations and substitutions (A) or using only GC-conservative mutations and substitutions (B). Group level π_s and life history traits are estimated by averaging species level estimates across closely related species. Black dotted lines represent significant regressions across taxonomic groups and grey dotted lines non-significant ones.

Figure S4: Relationship between species-level ω_{na} and π_s and $\log_{10}$ transformed life history traits.

ω_{na} is estimated using all mutations and substitutions (A) or using only GC-conservative mutations and substitutions (B). Black dotted lines represent significant regressions across taxonomic groups and grey dotted lines non-significant ones.

Figure S5: Relationship between species-level α and π_s.

α is estimated using all mutations and substitutions (A) or using only GC-conservative mutations and substitutions (B). The dotted line represents the regression across all species, and full lines represent the regression within each taxonomic groups. Black dotted lines represent significant regressions across taxonomic groups and grey dotted lines non-significant ones.

Figure S6: Design of the simulations of fluctuation of population size.

A: three fold ratio between low and high population size and high long-term population size.

B: thirty fold ratio between low and high population size and high long-term population size.

C: three fold ratio between low and high population size and low long-term population size.

D: thirty fold ratio between low and high population size and low long-term population size.

Figure S7: Relationship between ω_a and π_s in simulated scenarios of fluctuating population size.

A: three fold ratio between low and high population size and high long-term population size (scenario A in figure S1)

B: thirty fold ratio between low and high population size and high long-term population size (scenario B in figure S1)

C: three fold ratio between low and high population size and low long-term population size (scenario C in figure S1)

D: thirty fold ratio between low and high population size and low long-term population size (scenario D in figure S1)

References:

1. Bell G. Evolutionary rescue and the limits of adaptation. Philosophical Transactions of the Royal Society B: Biological Sciences. 2013;368(1610):20120080.

2. Lanfear R, Kokko H, Eyre-Walker A. Population size and the rate of evolution. Trends in Ecology & Evolution. janv 2014;29(1):33-41.

3. Smith JM. What Determines the Rate of Evolution? The American Naturalist. 1 mai 1976;110(973):331-8.

4. Nam K, Munch K, Mailund T, Nater A, Greminger MP, Krützen M, et al. Evidence that the rate of strong selective sweeps increases with population size in the great apes. Proceedings of the National Academy of Sciences. 14 févr 2017;114(7):1613-8.

5. Bürger R, Lynch M. Evolution and extinction in a changing environment: a quantitative-genetic analysis. Evolution. 1995;49(1):151-63.

6. Barton N, Partridge L. Limits to natural selection. BioEssays. 2000;22(12):1075-84.

7. Kopp M, Hermisson J. The genetic basis of phenotypic adaptation II: the distribution of adaptive substitutions in the moving optimum model. Genetics. 2009;183(4):1453-76.

8. Karasov T, Messer PW, Petrov DA. Evidence that Adaptation in Drosophila Is Not Limited by Mutation at Single Sites. PLOS Genetics. 17 juin 2010;6(6):e1000924.

9. Weissman DB, Barton NH. Limits to the Rate of Adaptive Substitution in Sexual Populations. PLOS Genetics. 7 juin 2012;8(6):e1002740.

10. Yeaman S, Gerstein AC, Hodgins KA, Whitlock MC. Quantifying how constraints limit the diversity of viable routes to adaptation. PLoS genetics. 2018;14(10):e1007717.

11. Huber CD, Kim BY, Marsden CD, Lohmueller KE. Determining the factors driving selective effects of new nonsynonymous mutations. Proceedings of the National Academy of Sciences. 2017;114(17):4465-70.

12. McDonald JH, Kreitman M. Adaptive protein evolution at the Adh locus in Drosophila. Nature. 20 juin 1991;351(6328):652-4.

13. Smith NGC, Eyre-Walker A. Adaptive protein evolution in *Drosophila*. Nature. févr 2002;415(6875):1022-4.

14. Keightley PD, Eyre-Walker A. Joint inference of the distribution of fitness effects of deleterious mutations and population demography based on nucleotide polymorphism frequencies. Genetics. 2007;177(4):2251-61.

15. Boyko AR, Williamson SH, Indap AR, Degenhardt JD, Hernandez RD, Lohmueller KE, et al. Assessing the evolutionary impact of amino acid mutations in the human genome. PLoS genetics. 2008;4(5):e1000083.

16. Eyre-Walker A, Keightley PD. Estimating the Rate of Adaptive Molecular Evolution in the Presence of Slightly Deleterious Mutations and Population Size Change. Mol Biol Evol. 1 sept 2009;26(9):2097-108.

17. Messer PW, Petrov DA. Frequent adaptation and the McDonald–Kreitman test. PNAS. 21 mai 2013;110(21):8615-20.

18. Galtier N. Adaptive Protein Evolution in Animals and the Effective Population Size Hypothesis. PLOS Genetics. 11 janv 2016;12(1):e1005774.

19. Keightley PD, Campos JL, Booker TR, Charlesworth B. Inferring the Frequency Spectrum of Derived Variants to Quantify Adaptive Molecular Evolution in Protein-Coding Genes of Drosophila melanogaster. Genetics. 1 juin 2016;203(2):975-84.

20. Tataru P, Mollion M, Glémin S, Bataillon T. Inference of Distribution of Fitness Effects and Proportion of Adaptive Substitutions from Polymorphism Data. Genetics. 1 nov 2017;207(3):1103-19.

21. Loewe L, Charlesworth B. Inferring the distribution of mutational effects on fitness in Drosophila. Biology Letters. 22 sept 2006;2(3):426-30.

22. Stoletzki N, Eyre-Walker A. Estimation of the neutrality index. Molecular biology and evolution. 2010;28(1):63-70.

23. Rousselle M, Mollion M, Nabholz B, Bataillon T, Galtier N. Overestimation of the adaptive substitution rate in fluctuating populations. Biology Letters. 1 mai 2018;14(5):20180055.

24. Eyre-Walker A. Changing effective population size and the McDonald-Kreitman test. Genetics. 2002;162(4):2017-24.

25. Corcoran P, Gossmann TI, Barton HJ, Slate J, Zeng K. Determinants of the Efficacy of Natural Selection on Coding and Noncoding Variability in Two Passerine Species. Genome Biol Evol. 1 nov 2017;9(11):2987-3007.

26. Rousselle M, Laverré A, Figuet E, Nabholz B, Galtier N. Influence of Recombination and GC-biased Gene Conversion on the Adaptive and Nonadaptive Substitution Rate in Mammals versus Birds. Mol Biol Evol [Internet]. [cité 22 févr 2019]; Disponible sur: https://academic.oup.com/mbe/advance-article/doi/10.1093/molbev/msy243/5261349

27. Bolívar P, Mugal CF, Rossi M, Nater A, Wang M, Dutoit L, et al. Biased inference of selection due to GC-biased gene conversion and the rate of protein evolution in flycatchers when accounting for it. Mol Biol Evol [Internet]. [cité 3 août 2018]; Disponible sur: https://academic.oup.com/mbe/advance-article/doi/10.1093/molbev/msy149/5063898

28. Ohta T. The Nearly Neutral Theory of Molecular Evolution. Annual Review of Ecology and Systematics. 1992;23(1):263-86.

29. Gossmann TI, Keightley PD, Eyre-Walker A. The Effect of Variation in the Effective Population Size on the Rate of Adaptive Molecular Evolution in Eukaryotes. Genome Biol Evol. 1 janv 2012;4(5):658-67.

30. Gossmann TI, Song B-H, Windsor AJ, Mitchell-Olds T, Dixon CJ, Kapralov MV, et al. Genome wide analyses reveal little evidence for adaptive evolution in many plant species. Molecular biology and evolution. 2010;27(8):1822-32.

31. Strasburg JL, Kane NC, Raduski AR, Bonin A, Michelmore R, Rieseberg LH. Effective population size is positively correlated with levels of adaptive divergence among annual sunflowers. Molecular biology and evolution. 2010;28(5):1569-80.

32. Lourenço JM, Glémin S, Galtier N. The rate of molecular adaptation in a changing environment. Molecular biology and evolution. 2013;30(6):1292-301.

33. Simion P, Belkhir K, François C, Veyssier J, Rink JC, Manuel M, et al. A software tool ‘CroCo’detects pervasive cross-species contamination in next generation sequencing data. BMC biology. 2018;16(1):28.

34. James JE, Piganeau G, Eyre-Walker A. The rate of adaptive evolution in animal mitochondria. Molecular ecology. 2016;25(1):67-78.

35. Galtier N, Roux C, Rousselle M, Romiguier J, Figuet E, Glémin S, et al. Codon Usage Bias in Animals: Disentangling the Effects of Natural Selection, Effective Population Size, and GC-Biased Gene Conversion. Molecular biology and evolution. 2018;35(5):1092-103.

36. Romiguier J, Gayral P, Ballenghien M, Bernard A, Cahais V, Chenuil A, et al. Comparative population genomics in animals uncovers the determinants of genetic diversity. Nature. 2014;515(7526):261.

37. Chen J, Glémin S, Lascoux M. Genetic Diversity and the Efficacy of Purifying Selection across Plant and Animal Species. Molecular Biology and Evolution. juin 2017;34(6):1417-28.

38. Zhen Y, Huber CD, Davies RW, Lohmueller KE. Stronger and higher proportion of beneficial amino acid changing mutations in humans compared to mice and flies. 26 sept 2018 [cité 10 oct 2018]; Disponible sur: http://biorxiv.org/lookup/doi/10.1101/427583

39. Eyre-Walker A, Woolfit M, Phelps T. The Distribution of Fitness Effects of New Deleterious Amino Acid Mutations in Humans. Genetics. 1 juin 2006;173(2):891-900.

40. Jensen JD, Bachtrog D. Characterizing the Influence of Effective Population Size on the Rate of Adaptation: Gillespie's Darwin Domain. Genome Biol Evol. 24 juin 2011;3:687-701.

41. Gillespie JH. IS THE POPULATION SIZE OF A SPECIES RELEVANT TO ITS EVOLUTION? - Gillespie - 2001 - Evolution - Wiley Online Library [Internet]. 2001 [cité 11 juill 2019]. Disponible sur: https://onlinelibrary.wiley.com/doi/abs/10.1111/j.0014-3820.2001.tb00732.x

42. Gillespie JH. The neutral theory in an infinite population. Gene. 2000;261(1):11-8.

43. Corbett-Detig RB, Hartl DL, Sackton TB. Natural Selection Constrains Neutral Diversity across A Wide Range of Species. PLOS Biology. 10 avr 2015;13(4):e1002112.

44. Coop G. Does linked selection explain the narrow range of genetic diversity across species? bioRxiv. 7 mars 2016;042598.

45. Enard D, Cai L, Gwennap C, Petrov DA. Viruses are a dominant driver of protein adaptation in mammals. :25.

46. Razeto-Barry P, Díaz J, Vásquez RA. The nearly neutral and selection theories of molecular evolution under the fisher geometrical framework: substitution rate, population size, and complexity. Genetics. 2012;191(2):523-34.

47. Orr HA. Adaptation and the Cost of Complexity. Evolution. 1 févr 2000;54(1):13-20.

48. Valentine JW, Collins AG, Meyer CP. Morphological complexity increase in metazoans. Paleobiology. 1994;20(2):131-42.

49. Stumpf MP, Thorne T, de Silva E, Stewart R, An HJ, Lappe M, et al. Estimating the size of the human interactome. Proceedings of the National Academy of Sciences. 2008;105(19):6959-64.

50. Fernández A, Lynch M. Non-adaptive origins of interactome complexity. Nature. 2011;474(7352):502.

51. Rousselle M, Faivre N, Ballenghien M, Galtier N, Nabholz B. Hemizygosity Enhances Purifying Selection: Lack of Fast-Z Evolution in Two Satyrine Butterflies. Genome Biol Evol. 1 oct 2016;8(10):3108-19.

52. Ballenghien M, Faivre N, Galtier N. Patterns of cross-contamination in a multispecies population genomic project: detection, quantification, impact, and solutions. BMC Biology [Internet]. déc 2017 [cité 12 mars 2018];15(1). Disponible sur: http://bmcbiol.biomedcentral.com/articles/10.1186/s12915-017-0366-6

53. Meyer M, Kircher M. Illumina sequencing library preparation for highly multiplexed target capture and sequencing. Cold Spring Harbor Protocols. 2010;2010(6):pdb. prot5448.

54. Tilak M-K, Justy F, Debiais-Thibaud M, Botero-Castro F, Delsuc F, Douzery EJP. A cost-effective straightforward protocol for shotgun Illumina libraries designed to assemble complete mitogenomes from non-model species. Conservation Genet Resour. 1 mars 2015;7(1):37-40.

55. Rohland N, Reich D. Cost-effective, high-throughput DNA sequencing libraries for multiplexed target capture. Genome research. 2012;

56. Bolger AM, Lohse M, Usadel B. Trimmomatic: a flexible trimmer for Illumina sequence data. Bioinformatics. 2014;30(15):2114-20.

57. Cahais V, Gayral P, Tsagkogeorga G, Melo-Ferreira J, Ballenghien M, Weinert L, et al. Reference-free transcriptome assembly in non-model animals from next-generation sequencing data. Molecular ecology resources. 2012;12(5):834-45.

58. Simpson JT, Wong K, Jackman SD, Schein JE, Jones SJ, Birol I. ABySS: a parallel assembler for short read sequence data. Genome research. 2009;19(6):1117-23.

59. Huang X, Madan A. CAP3: A DNA sequence assembly program. Genome research. 1999;9(9):868-77.

60. Grabherr MG, Haas BJ, Yassour M, Levin JZ, Thompson DA, Amit I, et al. Full-length transcriptome assembly from RNA-Seq data without a reference genome. Nature biotechnology. 2011;29(7):644.

61. Li H, Durbin R. Fast and accurate short read alignment with Burrows–Wheeler transform. Bioinformatics. 2009;25(14):1754-60.

62. Tsagkogeorga G, Cahais V, Galtier N. The population genomics of a fast evolver: high levels of diversity, functional constraint, and molecular adaptation in the tunicate Ciona intestinalis. Genome Biology and Evolution. 2012;4(8):852-61.

63. Gayral P, Melo-Ferreira J, Glémin S, Bierne N, Carneiro M, Nabholz B, et al. Reference-free population genomics from next-generation transcriptome data and the vertebrate–invertebrate gap. PLoS genetics. 2013;9(4):e1003457.

64. Ranwez V, Delsuc F, Ranwez S, Belkhir K, Tilak M-K, Douzery EJ. OrthoMaM: a database of orthologous genomic markers for placental mammal phylogenetics. BMC evolutionary biology. 2007;7(1):241.

65. Douzery EJ, Scornavacca C, Romiguier J, Belkhir K, Galtier N, Delsuc F, et al. OrthoMaM v8: a database of orthologous exons and coding sequences for comparative genomics in mammals. Molecular biology and evolution. 2014;31(7):1923-8.

66. Emms DM, Kelly S. OrthoFinder: solving fundamental biases in whole genome comparisons dramatically improves orthogroup inference accuracy. Genome biology. 2015;16(1):157.

67. Ranwez V, Harispe S, Delsuc F, Douzery EJ. MACSE: Multiple Alignment of Coding SEquences accounting for frameshifts and stop codons. PloS one. 2011;6(9):e22594.

68. Guéguen L, Gaillard S, Boussau B, Gouy M, Groussin M, Rochette NC, et al. Bio++: efficient extensible libraries and tools for computational molecular evolution. Molecular biology and evolution. 2013;30(8):1745-50.

69. Haller BC, Messer PW. SLiM 2: Flexible, Interactive Forward Genetic Simulations. Mol Biol Evol. 1 janv 2017;34(1):230-40.